The jaw is a second-class lever in *Pedetes capensis* (Rodentia: Pedetidae)

Philip G Cox Corresp. 1, 2

1 Department of Archaeology, University of York, York, UK

2 Hull York Medical School, University of York, York, UK

Corresponding Author: Philip G Cox
Email address: philip.cox@hyms.ac.uk

The mammalian jaw is often modelled as a third-class lever for the purposes of biomechanical analyses, owing to the position of the resultant muscle force between the jaw joint and the teeth. However, it has been proposed that in many rodents, the jaws operate as a second-class lever during distal molar bites, owing to the rostral position of the masticatory musculature. In particular, the infraorbital portion of the zygomatico-mandibularis (IOZM) has been suggested to be of major importance in converting the masticatory system from a third-class to a second-class lever. The presence of the IOZM is diagnostic of the hystricomorph rodents, and is particularly well-developed in *Pedetes capensis*, the South African springhare. In this study, finite element analysis (FEA) was used to assess the lever mechanics of the springhare masticatory system, and to determine the function of the IOZM. An FE model of the skull of *P. capensis* was constructed and loaded with all masticatory muscles, and then solved for biting at each tooth in turn. Further load cases were created in which each masticatory muscle was removed in turn. The analyses showed that the mechanical advantage of the springhare jaws was above one at all molar bites and very close to one during the premolar bite. Removing the IOZM or masseter caused a drop in mechanical advantage at all bites, but affected strain patterns and cranial deformation very little. Removing the ZM had only a small effect on mechanical advantage, but produced a substantial reduction in strain and deformation across the skull. It was concluded that the masticatory system of *P. capensis* acts as a second class lever during bites along almost the entire cheek tooth row. The IOZM is clearly a major contributor to this effect, but the masseter also has part to play. The benefit of the IOZM is that it adds force without substantially contributing to strain or deformation of the skull. This may help explain why the hystricomorphous morphology has evolved multiple times independently within Rodentia.

1 **The jaw is a second-class lever in *Pedetes capensis* (Rodentia: Pedetidae)**

3 Philip G. Cox[1,2]

4 [1]Department of Archaeology, University of York, York, YO10 5DD, UK

5 [2]Hull York Medical School, University of York, York, YO10 5DD, UK

7 Corresponding author:

8 Philip G. Cox

9 Email: philip.cox@hyms.ac.uk

32   **ABSTRACT**

33   The mammalian jaw is often modelled as a third-class lever for the purposes of biomechanical

34   analyses, owing to the position of the resultant muscle force between the jaw joint and the teeth.

35   However, it has been proposed that in many rodents, the jaws operate as a second-class lever

36   during distal molar bites, owing to the rostral position of the masticatory musculature. In

37   particular, the infraorbital portion of the zygomatico-mandibularis (IOZM) has been suggested to

38   be of major importance in converting the masticatory system from a third-class to a second-class

39   lever. The presence of the IOZM is diagnostic of the hystricomorph rodents, and is particularly

40   well-developed in *Pedetes capensis*, the South African springhare. In this study, finite element

41   analysis (FEA) was used to assess the lever mechanics of the springhare masticatory system, and

42   to determine the function of the IOZM. An FE model of the skull of *P. capensis* was constructed

43   and loaded with all masticatory muscles, and then solved for biting at each tooth in turn. Further

44   load cases were created in which each masticatory muscle was removed in turn. The analyses

45   showed that the mechanical advantage of the springhare jaws was above one at all molar bites

46   and very close to one during the premolar bite. Removing the IOZM or masseter caused a drop in

47   mechanical advantage at all bites, but affected strain patterns and cranial deformation very little.

48   Removing the ZM had only a small effect on mechanical advantage, but produced a substantial

49   reduction in strain and deformation across the skull. It was concluded that the masticatory system

50   of *P. capensis* acts as a second class lever during bites along almost the entire cheek tooth row.

51   The IOZM is clearly a major contributor to this effect, but the masseter also has part to play. The

52   benefit of the IOZM is that it adds force without substantially contributing to strain or

53   deformation of the skull. This may help explain why the hystricomorphous morphology has

54   evolved multiple times independently within Rodentia.

55

56

57

58

59

60

61

62

63 **INTRODUCTION**

64 The mammalian jaw is frequently treated as a lever for the purposes of biomechanical analysis

65 (e.g. Crompton, 1963; Bramble, 1978; Greaves, 1978, 1982, 2000; Gingerich, 1979; Thomason,

66 1991; Satoh, 1998; 1999; Spencer, 1998, 1999; Satoh & Iwaku, 2006, 2009; Davis et al., 2010;

67 Druzinsky, 2010; Cornette et al., 2012; Becerra et al., 2013; Santana, 2015). More specifically, it

68 is frequently considered to be a third-class lever i.e. one in which the input force sits between the

69 fulcrum and the output force (Kerr, 2010). In mammals, the resultant masticatory muscle force

70 (the input force) is usually situated between the jaw joint (fulcrum) and the biting tooth (output

71 force) and thus the comparison with a third-class lever is generally accurate. The advantage of

72 positioning muscle force posterior to the teeth is that relatively wide gapes can be achieved and

73 high tensile forces at the temporo-mandibular joint, which could lead to dislocation of the jaws,

74 are avoided (Greaves, 2000, 2012). However, the trade-off is that the mechanical advantage of a

75 third-class lever is always less than one – that is, the output bite force will always be less than the

76 effective muscle force.

77

78 It has occasionally been proposed that mammalian jaws do not always operate as third-class

79 levers (Davis, 1955; Turnbull, 1970), and can in certain circumstances act as second-class levers

80 with the output force between fulcrum and input force. In his classic work on the mammalian

81 masticatory system, Turnbull (1970) suggested that the relative size and position of the masseter

82 in many rodents (and a few ungulates) can shift the resultant of the masticatory musculature

83 anterior to the distal cheek teeth, converting the masticatory system into a second-class lever

84 during distal molar biting. Such an effect has even been claimed to occur in humans, with the

85 jaw operating as a second-class lever during bites on the second and third molars (Mansour &

86 Reynik, 1975). Alternatively, other authors have argued that although some parts of the muscle

87 mass attach far forward on the jaws in rodents, the resultant muscle force is still located towards

88 the posterior end of the jaw (Greaves, 2012).

89

90 In rodents, one muscle in particular has been identified as contributing to the jaw operating as a

91 second-class lever. The infraorbital portion of the zygomatico-mandibularis (IOZM) is an

92 anterior expansion of the deepest layer of the masseter, the zygomatico-mandibularis (ZM),

93 which passes through the enlarged infraorbital foramen to take its origin on the lateral surface of

94   the rostrum. The IOZM, also referred to as the maxillo-mandibularis (Becht, 1953; Turnbull,

95   1970) or medial masseter (Wood, 1965; Woods, 1972), is the one of the defining characters of

96   hystricomorph rodents, but is also present in a somewhat smaller form in myomorphs, where it is

97   found in combination with a rostral expansion of the deep masseter (Wood, 1965; Cox & Jeffery,

98   2011). Given its rostral origin on the skull and its mandibular insertion at the level of the

99   premolar, Becht (1953) believed the function of the IOZM was to convert the jaw from a third-

100 class lever to a second-class lever during molar biting.

101

102 This study seeks to understand the lever mechanics of the skull in the South African springhare,

103 *Pedetes capensis* – a rodent species in which the IOZM is notably well-developed (Offermans &

104 De Vree, 1989). *P. capensis* is a nocturnal, bipedal, saltatorial rodent that inhabits arid and semi-

105 arid areas of southern Africa (Peinke & Brown, 2003). It is large for a rodent (3-4 kg) and feeds

106 principally on grasses, especially the rhizomes of *Cynodon dactylon* and the tubers of *Cyperus*

107 *esculentus* (Peinke & Brown, 2006). *P. capensis* and its sister-species *P. surdaster* are the only

108 two extant members of the Pedetidae (Wilson & Reeder, 2005), a family which molecular

109 analyses place as sister-group to the Anomaluridae (scaly-tailed flying squirrels) in the

110 Anomaluromorpha, which itself is part of the mouse-related clade (Fabre et al., 2012). Given the

111 presence of the IOZM muscle, the pedetids (and anomalurids) have been identified as being

112 hystricomorphous (Wood, 1965). However, the hystricomorphy seen in the Anomaluromorpha

113 has evolved independently from that seen in three other groups of rodents: the Ctenohystrica, the

114 Dipodidae, and some members of the Gliridae (Hautier, Cox & Lebrun, 2015). Thus, the

115 function of the IOZM is of prime interest to understanding the evolution of the rodents – why has

116 this muscle arisen independently so many times throughout rodents?

117

118 The aim of this study is to model the masticatory system of *P. capensis* to determine if it

119 functions as a second or third-class lever, and to assess the function of the masticatory muscles,

120 particularly the IOZM. There are two specific hypotheses that will be tested:

121   1. It is hypothesised that a model of the skull of *P. capensis* will demonstrate the

122   masticatory system operating as a second-class lever along most of the molar tooth row.

123   This is expected based on previous dissection work by Offermans and De Vree (1989)

124   who showed that a great deal of the masticatory musculature is situated alongside or

anterior to the cheek teeth. The masticatory system will be determined to be a second-class lever when the bite force exceeds the effective muscle force, i.e. when the mechanical advantage is greater than one, and when the reaction force at the temporo-mandibular joint is negative.

2. It is hypothesised that the IOZM muscle has a major role in converting the masticatory system from a third to a second-class lever in *P. capensis*. This hypothesis was previously proposed by Becht (1953) and is also expected owing to the large size and rostral position of the IOZM (Offermans & De Vree, 1989, 1993). The function of the IOZM will be determined by virtual ablation analyses i.e. removing it and other muscles from the models to elucidate the effect on the biomechanical performance of the system, as determined by mechanical advantage, principal strains and the overall deformation of the skull during biting.

Previous studies of the lever mechanics of the mammalian masticatory system have tended to focus on the mandible (Greaves, 1978; 1982, 2000; Spencer, 1998, 1999), owing to its relatively simple shape and because its function is largely limited to feeding. However, in this study, the skull will be analysed, because of the interest in the IOZM, which has a particularly unusual fan-shaped origin on the rostrum. To address the hypotheses and to study the function of the springhare skull during biting, finite element analysis (FEA) will be employed. FEA is an engineering technique for predicting stress, strain and deformation in an object during loading (Rayfield, 2007), and is now frequently applied to reconstructions of skulls and other skeletal elements in order to analyse vertebrate biomechanics (e.g. Richmond et al., 2005; Kupczik et al., 2007; Dumont et al., 2011; Ross et al., 2011; Cox et al., 2012; Cox, Kirkham & Herrel, 2013; O'Hare et al., 2013; Porro et al., 2013; Figueirido et al., 2014; Cuff, Bright & Rayfield, 2015; Sharp, 2015; McIntosh & Cox, 2016; McCabe et al., 2017; Tsouknidas et al., 2017). As well as simulating stress and strain distributions, FEA is also able to predict reaction forces, and so will be used here to estimate bite force, jaw joint reaction force and mechanical advantage. Although these metrics could in theory be estimated via simple 2D lever models, it has been shown that such simplification leads to inaccuracies in muscle attachment areas, force magnitudes and directions of pull (Davis et al., 2010; Greaves, 2012). The advantage of FEA is that muscle forces can be distributed across the whole attachment site rather than being modelled as

156   originating from a single centroid point, and muscle force vectors can act in three dimensions
157   rather than two.

158

159   **MATERIALS AND METHODS**

160   **Sample and model creation**

161   The cranium and mandible of an adult specimen of *Pedetes capensis*, the South African
162   springhare, were obtained from the University Museum of Zoology, Cambridge (catalogue
163   number E.1446). The sex of the specimen was unknown, but sexual dimorphism has not been
164   reported in this species (Offermans & De Vree, 1989; López-Antoñanzas, 2016). The specimen
165   was microCT scanned on the X-Tek Metris system in the Medical and Biological Engineering
166   group, University of Hull. Voxels were isometric with dimensions of 0.052 mm and 0.041 mm
167   for the cranium and mandible respectively.

168

169   A virtual reconstruction of the cranium was created from the scan using Avizo 8 (FEI, Hillsboro,
170   OR). Bone and teeth were segmented as separate materials, but no differentiation was made
171   between cortical and trabecular bone, nor between different materials within the teeth. These
172   simplifications of the model geometry were felt to be justified as several previous studies have
173   indicated that, whilst absolute strain magnitudes are impacted by the presence or absence of
174   trabecular bone and different tooth materials, the large-scale patterns of deformation are
175   relatively insensitive to such changes (Fitton et al., 2015; Toro-Ibacache et al., 2016). In order to
176   reduce solution times and allow effective manipulation of the model in the FE software, the
177   reconstruction was down-sampled to a voxel size of 0.21 x 0.21 x 0.21 mm. The cranial
178   reconstruction was then converted into a mesh of 2310268 eight-noded, cubic (first-order)
179   elements via direct voxel conversion, implemented in VOX-FE, custom-built open-source FE
180   software (Liu et al., 2012). The Avizo reconstruction and VOX-FE model are both available for
181   download at https://figshare.com/articles/Springhare_FEA/5082598.

182

183   **Material properties, constraints and loads**

184   Material properties were assigned to the model based on previous nano-indentation work on
185   rodent skulls (Cox et al., 2012). Both bone and teeth were assumed to be linearly elastic isotropic
186   with Young's moduli of 17 and 30 GPa respectively and a Poisson's ratio of 0.3 for both. The

187   model was constrained at both temporo-mandibular joints as well as the biting tooth. The jaw

188   joints were constrained in all three dimensions, whilst the bite points were only constrained in

189   the bite direction (i.e. orthogonal to the occlusal plane). This configuration of constraints is

190   somewhat conservative (it restricts the jaw to simple hinge movements), but has been used by a

191   number of other authors previously (Porro et al., 2013; Cuff, Bright & Rayfield, 2015; Cox,

192   Rinderknecht & Blanco, 2015) and provides robust conclusions with regard to mechanical

193   advantage. The number of nodes constrained at each location varied between 158 and 332.

194

195   Loads were applied to both sides of the model to simulate the following jaw-closing muscles (see

196   Figure 1) based on previous published data (Offermans & De Vree, 1989, 1993): masseter

197   (combining the superficial and deep layers), posterior masseter, ZM, IOZM, temporalis, medial

198   pterygoid and lateral pterygoid. Unfortunately, the superficial and deep masseters could not be

199   modelled separately, because they were recorded as a single entity in Offermans & De Vree

200   (1993). Muscle attachment sites were determined based on the detailed descriptions and figures

201   in Offermans & De Vree (1989). Muscle directions of pull were assigned using landmarks

202   recorded from the insertion areas on a reconstruction of the springhare mandible, created from

203   the previously gathered microCT scans. Muscle forces were calculated by multiplying the

204   physiological cross-sectional areas (PCSA) given in Offermans & De Vree (1993) by an intrinsic

205   muscle stress value of 0.3 Nmm^{-2} (van Spronsen et al., 1989; Sharp, 2015; Tseng & Flynn,

206   2015). These muscle forces were then modified based on the maximum percentage activations

207   recorded by electromyography during incision and mastication of groundnuts (Offermans &

208   DeVree, 1993). Thus the relative proportions of total muscle force provided by each muscle were

209   different in incisor biting to premolar/molar biting. Applied muscle forces for incision and

210   mastication are given in Table 1. In order to ascertain the function of the masticatory muscles,

211   versions of the model were created without each of the muscles in turn. The loaded FE model is

212   shown in Figure 1.

213

214   **Model solution and analysis**

215   The model was solved for biting at each tooth along the dental arcade. Based on experimental

216   work by Offermans & De Vree (1990), all bites were modelled as bilateral i.e. the muscles on

217   both sides of the skull were active with identical forces and the same tooth was loaded on each

218 side of the dental row. Reaction forces at the biting tooth and at the jaw joints were calculated for
219 each loadcase. Bite forces were divided by the effective muscle force (equal to the sum of the
220 bite force and joint reaction forces) to calculate the mechanical advantage of the masticatory
221 system at each tooth. As a ratio, the mechanical advantage provides a useful metric for
222 comparing loadcases with different input muscle forces. It should be noted that it is a different
223 measure to the mechanical efficiency of biting used in other studies (Dumont et al., 2011; Cox et
224 al., 2012; Cox, Kirkham & Herrel, 2013), which divides the bite force by the total adductor
225 muscle force, but does not take into account the orientation of muscle vectors. The distribution of
226 maximum (ε_1: predominantly tensile) and minimum (ε_3: predominantly compressive) principal
227 strains across the skull were examined using contour maps. Geometric morphometric methods
228 were used to analyse deformation patterns across the skull (Cox et al., 2011; Cox, Kirkham &
229 Herrel, 2013; O'Higgins et al., 2011; McIntosh & Cox, 2016). A set of 46 3D landmark co-
230 ordinates (described in Figure 2 and Table S1), based on that used in Cox, Kirkham & Herrel
231 (2013), was recorded from each solved model as well as from the original unloaded model. As
232 changes in size are of equal significance to changes in shape during mechanical loading, the
233 landmark sets were subjected to a Procrustes size and shape analysis (O'Higgins & Milne, 2013),
234 not a Procrustes form analysis, which gives a lower weighting to size (Fitton et al., 2015). This
235 was followed by a principal component analysis (PCA). All analyses were implemented in the
236 EVAN toolbox software (www.evan-society.org).

237

238 **RESULTS**
239 The absolute bite forces and joint reaction forces predicted by the model during biting at each
240 tooth in *P. capensis* are given in Table 2. In addition, the mechanical advantage of the jaws at
241 each bite has been calculated. It can be seen that joint reaction forces are negative and
242 mechanical advantage exceeds one at all three molar teeth. In addition, the mechanical advantage
243 is almost one (0.99) and the joint reaction force is close to zero (2.8 N) at the premolar.

244

245 The effect of removing each of the masticatory muscles on the overall mechanical advantage is
246 given in Table 2 and shown in Figure 3. Removal of either the IOZM or the masseter causes a
247 decrease in mechanical advantage during both incision and mastication, with removal of the
248 IOZM leading to the greatest decrease. Removal of the medial pterygoid muscle leads to an

249   increase in mechanical advantage across all cheek teeth, but little effect is seen during incisor

250   biting. Removal of the ZM causes a substantial drop in bite force at all teeth, but has little effect

251   on the mechanical advantage of the system, except at the incisor where mechanical advantage

252   increases in the absence of the ZM. Removal of the posterior masseter, temporalis or lateral

253   pterygoid results in very little change in either bite force or mechanical advantage at any of the

254   teeth, and hence the results of the models lacking these muscles have not been illustrated in

255   Figure 3.

256

257   The contour maps of principal strain distribution across the cranium of *P. capensis* during biting

258   on the incisor and first molar are shown in Figure 4. It can be seen that the highest maximum and

259   minimum principal strains are concentrated in similar areas of the skull – along the zygomatic

260   arch and up its wide ascending ramus, and across the orbital wall, especially the anterior part.

261   However, there are some differences between the strain distributions. The ascending ramus of

262   the zygomatic arch is subject to greater ε_1 strains than ε_3 strains, and thus is predominantly under

263   tension, whereas the orbital wall seems to be experiencing greater ε_3 strains and is likely mostly

264   in compression. Strains are generally greater during molar biting than incision, and there is an

265   overall caudal shift of the most highly strained regions away from the rostrum towards the orbit

266   as the bite point moves posteriorly along the tooth row.

267

268   Figure 4 also shows the effect of removing three of the masticatory muscles (IOZM, masseter

269   and ZM) on principal strain distributions. Despite being relatively large muscles, the impact of

270   removing the IOZM or the masseter appears to be minimal. There are very few differences

271   between models with all masticatory muscles applied and those without the IOZM, except for a

272   slight reduction in strain on the rostrum and in the posterior part of the orbit during incisor and

273   molar biting. Removal of the masseter has little effect on the strains generated by incisor biting,

274   but reduces strains across the zygomatic arch and in the anterior part of the orbit during molar

275   biting. Elimination of the ZM from the model, however, leads to a substantial reduction in ε_1 and

276   ε_3 strains across the skull during bites at all teeth.

277

278   The geometric morphometric analysis highlights differences in the magnitude and mode of

279   deformation between the different loadcases solved in this study. Figure 5 shows the scatter plot

280   of the first two principal components. The first principal component encompasses 90% of the

281   variation, and the second principal component 9% of the variation. It should be noted that to be

282   able to visualise change across PC2, the axes have not been shown to the same scale. As

283   demonstrated by the warped reconstructions in Figure 5, the shape change along PC1 is mainly

284   bending of the zygomatic arch, and this axis mostly separates loaded models from the unloaded

285   skull, incisor bites from bites on other teeth, and models with different muscles excluded from

286   one another. In general, incisor bites result in smaller deformations than cheek tooth bites (that

287   is, the incisor bites are found closer to the unloaded model on PC1), whereas premolar and molar

288   bites produce very similar deformations. Models lacking the IOZM, temporalis, medial pterygoid

289   or lateral pterygoid deform in a very similar manner to the models with all masticatory muscles,

290   whereas removal of the posterior masseter reduces the magnitude of deformation very slightly.

291   Removal of the masseter causes a greater reduction in cranial deformation and elimination of the

292   ZM (the largest masticatory muscle) causes the largest reduction in deformation. Shape change

293   along PC2 represents dorso-ventral bending of the skull and separates the four different bites

294   along the cheek tooth row.

295

296   **DISCUSSION**

297   The results of this study support both of the hypotheses proposed here. The skull of *Pedetes*

298   *capensis* operates as a second-class lever during biting along almost all of the cheek teeth (first

299   hypothesis), and this effect can be largely ascribed to the presence of the IOZM muscle (second

300   hypothesis), although the masseter is important in this regard as well.

301

302   *Second-class vs third-class lever*

303   The FE model of *P. capensis* indicates that the mechanical advantage of the masticatory system

304   is greater than one and the reaction forces at the temporo-mandibular joints are negative during

305   bites on all three molars. Furthermore, the mechanical advantage is almost one and the joint

306   reaction force is very close to zero during premolar biting. Thus, as the bite point moves distally

307   along the tooth row, the system switches from a third-class to a second-class lever somewhere

308   between the premolar and first molar. In an analysis of the mandibles of two murid species,

309   *Apodemus speciosus* and *Cleithrionomys rufocanus*, such an effect was calculated to occur

310   between the first and second molars (Satoh, 1999). The more anterior position of the effective

311   muscle force in the springhare may be driven in large part by its unusual cranial morphology. In
312   most hystricomorph rodents, the anterior root of the zygomatic arch arises from the skull
313   approximately at the level of the first cheek tooth, but in *P. capensis* it is much further forward,
314   attaching to the shortened rostrum just posterior to the maxillary incisor (Offermans & De Vree,
315   1989). Thus, the masticatory musculature, as a whole, is more rostrally positioned than in most
316   other rodents, and so the jaw becomes a second-class lever at more anterior position along the
317   tooth row.

318

319   The prediction of large tensile forces at the jaw joints of the springhare is a result that is at odds
320   with some published work on mammalian masticatory biomechanics. It has been argued that the
321   capsule and ligaments of the mammalian jaw joint are poorly suited to resisting high tensile
322   forces (Greaves, 2000, 2012), and that the mammalian masticatory system has evolved to
323   maintain the resultant muscle force within the posterior third the jaw ramus in order to prevent
324   instability and dislocation of the jaws (Greaves, 1978, 1982, 2000; Spencer, 1998, 1999). The
325   mismatch between the results presented here and this earlier work, may be the product of
326   insufficient knowledge of muscle recruitment in springhare mastication and also the limitations
327   of static FE models. Although the muscle forces were based on *in vivo* work that measured the
328   degree to which each muscle was activated during biting (Offermans & De Vree, 1993), a single
329   set of values was used for all molar bites; the only variation in muscle recruitment was between
330   incisor and cheek teeth bites. It has been shown that muscle recruitment can vary a great deal
331   from tooth to tooth, and even between bites on the same tooth (Cleuren, Aerts & De Vree, 1995).
332   Furthermore, the percentage activations used to calculate muscle force are the maximum applied
333   at any point during the masticatory cycle. Obviously, the recruitment of each muscle changes as
334   the teeth are brought into and out of occlusion, but a static model cannot reflect this. Thus, the
335   results here indicate that jaw is a second-class lever in molar biting, but this only holds true for
336   the muscle recruitment pattern applied to the model. In reality, the springhare may modulate
337   fibre recruitment within its complex set of muscles to maintain the jaws as a third-class lever
338   even at the distal molars. For instance, the external pterygoid may increase in activation during
339   distal molar biting to resist dislocation of the jaws as has been suggested to occur in murids
340   (Satoh, 1999).

341

342   Even after taking the limitations of the model into consideration, it is clear that the springhare is
343   has the potential to generate very high bite forces at its molar teeth. Moreover, even if not quite a
344   second-class lever these bites are efficient, so high bite forces can be produced without having to
345   massively increase the overall adductor muscle mass. It is likely that *P. capensis* has evolved this
346   highly efficient feeding system in order to cope with the demands of the arid environment in
347   which it lives (Peinke & Brown, 2003). Springhares are herbivorous, feeding almost exclusively
348   on grasses (Peinke & Brown, 2006). Although they are known to eat the leaves, springhares tend
349   to favour underground storage organs, such as rhizomes and tubers, particularly during autumn
350   and winter when nutritional reserves are transferred away from leaves and into the leaf bases and
351   roots (Peinke & Brown, 2006). These storage organs tend to be mechanically demanding to eat,
352   requiring a great deal of mastication to break down, which may have driven the evolution of the
353   highly efficient masticatory system of springhares. The disadvantage of the masticatory
354   arrangement seen in *P. capensis* is that the rostral position of many of the jaw-closing muscles is
355   likely to severely limit maximum gape. However, given their preferred diet of grasses, these
356   limitations are not likely to impact the ability of springhares to feed effectively.

357

358   *Function of the masticatory muscles*
359   The virtual ablation experiments, in which masticatory muscles were sequentially removed from
360   the FE model, show that the IOZM is the most important muscle in converting the masticatory
361   system from a third-class to second-class lever in molar biting, as predicted by the second
362   hypothesis. When the IOZM is removed, the mechanical advantage decreases, indicating that
363   more force is being directed towards the jaw joints. This has the effect that the point at which the
364   system switched from operating as a third-class to a second-class lever moves back to
365   somewhere between the first and second molars. Thus, this result supports the idea proposed by
366   Becht (1953) that the function of the IOZM is to convert the masticatory system to a second-
367   class lever during molar biting, at least in *P. capensis*. Removal of the IOZM had very little
368   impact on the distribution and magnitudes of strain across the skull (Figure 4), nor did it greatly
369   change the overall deformation of the skull during biting (Figure 5), as has also been noted in
370   another species of rodent, *Laonastes aenigmamus* (Cox, Kirkham & Herrel, 2013). Thus, it
371   appears that the increase in mechanical advantage gained by the presence of an IOZM muscle
372   does not come at the cost of greatly increased strain or deformation, either in the region of the

373   IOZM origin or elsewhere on the skull. In addition, the development of the IOZM in *P. capensis*

374   may be a response to the need to generate large forces at the incisors, such as during the cracking

375   of nutshells (Offermans & De Vree, 1990). The anterior position of the IOZM on the skull means

376   that improvements in incisor bite force can be achieved without an excessive increase in muscle

377   size.

378

379   The ZM is one of the largest masticatory muscles in the springhare (Offermans & De Vree,

380   1993), which is unusual among rodents; usually the ZM is smaller than the superficial and deep

381   masseters and the IOZM (Turnbull, 1970; Woods, 1972; Cox & Jeffery, 2011; Baverstock,

382   Jeffery & Cobb, 2013; Becerra et al., 2014). Despite its large size, the removal of the ZM from

383   the FE model had very little effect on the efficiency of the masticatory system i.e. the mechanical

384   advantage and joint reaction force remained largely the same. Thus, by virtue of being large, the

385   ZM is an important muscle for increasing overall bite force, but its presence does not alter the

386   efficiency of the system a great deal. However, the ZM does have a large effect on the

387   deformation of the springhare skull during biting. The GMM analysis showed that elimination of

388   the ZM greatly reduces the magnitude of deformation experienced by the skull (Figure 5), much

389   more so than any other masticatory muscle. This appears to be a consequence of the attachment

390   site of the ZM on the zygomatic arch. As has been found in other FEA studies of mammal skulls

391   (Bright, 2012; Cox et al., 2012; Fitton et al., 2012), the morphology of the zygomatic arch makes

392   it susceptible to larger deformations than other parts of the skull. Indeed, in this study,

393   deformations of the zygoma overwhelm deformations in all other parts of the skull, as can be

394   seen from the warped reconstructions in Figure 5. The large size and location of the ZM in *P.*

395   *capensis* leads to it being the principal generator of zygomatic strain and deformation. This can

396   be seen in Figure 4, where removal of the ZM vastly reduces strain in the zygomatic arch.

397

398   It has been suggested that the large zygomatic strains seen in many FEA studies of mammalian

399   skulls may be artificial and the result of a failure to incorporate important soft tissue structures

400   into the models. In particular, the temporal fascia has been shown to resist inferior bending of the

401   zygomatic arch in an FE model of a macaque (Curtis et al., 2011). This is unlikely to be the case

402   here as no temporal fascia was reported by Offermans & De Vree (1989) in their dissection of a

403   springhare. Furthermore, the temporalis is extremely small in *P. capensis*, and the temporal

404   region is positioned distinctly caudal the zygomatic arch, which would reduce the ability of a

405   temporal fascia to counteract ventral deflection of the zygomatic arch. However, there is an

406   aponeurosis attached extensively around the margin of the infraorbital fossa (Offermans & De

407   Vree, 1989), which may have the potential to resist some bending in the anterior part of the

408   zygomatic arc and its ascending ramus. Further work, both *ex vivo* dissection and *in silico*

409   modelling, is necessary to understand the biomechanical consequence of this aponeurosis.

410

411   The masseter has been shown to have a similar effect to the IOZM with regard to bite force,

412   although not quite to the same extent. It, too, appears to shift the resultant masticatory muscle

413   force anteriorly along the rostrum, thus directing force towards the biting tooth and away from

414   the jaw joints. Removal of the masseter has much the same effect as removing the IOZM – the

415   mechanical advantage is decreased and the point at which the system becomes a second-class

416   lever is shifted posteriorly along the tooth row. Unfortunately for this study, Offermans &

417   DeVree (1993) did not separate the superficial and deep masseter when measuring PCSA, so the

418   two muscles could not be modelled separately in the FEA. However, the illustrations in

419   Offermans & DeVree (1989) indicate that the fibres of the superficial masseter have a more

420   horizontal alignment than those of the deep masseter (as in most rodents, e.g. Turnbull, 1970), so

421   it is likely that the superficial masseter is the more important division of the masseter with regard

422   to the operation of the jaw as a second-class lever. In terms of cranial deformations, the masseter

423   has a similar, but lesser, effect to the ZM. Owing to its attachment to the zygomatic arch, the

424   action of the masseter generates inferior bending of the arch, and thus its removal tends to reduce

425   global deformation of the springhare cranium (Figure 5). It can also be seen that that removal of

426   the masseter causes a slight reduction in zygomatic and orbital strains during molar biting

427   (Figure 4).

428

429   The medial pterygoid, because of its posterior line of action, tends to direct muscle force away

430   from the teeth and towards the jaw joints, unlike the IOZM and masseter. Thus removal of the

431   medial pterygoid increased the mechanical advantage of the masticatory system. Overall, the

432   presence of the medial pterygoid increases bite force because it increases the total input adductor

433   muscle force, but it does so in a somewhat inefficient manner. Thus, although the medial

434   pterygoid has a relatively large PCSA, it has a relatively small effective muscle force owing to

435 its orientation. However, it has been shown that the medial pterygoid is important in other

436 aspects of masticatory biomechanics, notably as a counterbalance to the lateral pull of the

437 masseter, thereby preventing wishboning of the mandible (eversion of the lower border and

438 angular process) and reducing tensile strains at the symphysis (Hiiemae, 1971; Satoh, 1998; Cox

439 & Jeffery, 2015).

440

441 The posterior masseter, temporalis and lateral pterygoid are very small compared to the other

442 masticatory muscles in *P. capensis*, each providing less than 11% of the total adductor muscle

443 force. Hence, the impact of their removal on bite force and mechanical advantage was minimal.

444 Similarly, removal of these muscles had a very limited impact on the overall deformation of the

445 skull (Figure 5). The models without the temporalis and lateral pterygoid can barely be

446 distinguished from the models with all masticatory muscles. The models without a posterior

447 masseter show a very slight reduction in the magnitude of cranial deformation. This is because

448 the posterior masseter attaches to the caudal part of the zygomatic arch and thus is able to cause a

449 small amount of posterior deflection. It is likely that these muscles contribute to aspects of the

450 masticatory process other than bite force generation, especially the antero-posterior movements

451 of the mandible relative to the skull that are common to rodents. The temporalis, whilst clearly

452 too small to be a powerful elevator of the jaw as in myomorphs (Hiiemae, 1971; Gorniak, 1977),

453 may have a braking role during the power stroke of chewing (Byrd, 1981), and the lateral

454 pterygoid may be important in protraction of the mandible (Weijs & Dantuma, 1975; Gorniak,

455 1977) or in resisting tensile forces at the temporo-mandibular joint as mentioned above (Satoh,

456 1999).

457

458 **CONCLUSIONS**

459 The masticatory system of *P. capensis* has been shown to act as a second-class lever along the

460 majority of the cheek tooth row and, as predicted by Becht (1953), the IOZM is a particularly

461 important muscle in the switch from third-class to second-class lever mechanics. It should be

462 noted that masseter also plays an important role in this regard. This analysis of muscle function

463 is, of course, specific to *P. capensis* and further analyses of other species are necessary to

464 determine whether the conclusions hold true for other rodents. However, the position of the

465 IOZM, far forward on the rostrum, makes it likely that it will have some role to play in

466 increasing the mechanical advantage of the masticatory system in most hystricomorph rodents
467 (the exact scale of the effect being dependent on the size of the IOZM relative to the other
468 masticatory muscles). Previous research has suggested that, amongst rodents, sciuromorphs are
469 adapted for efficient gnawing at the incisors, whereas hystricomorphs are adapted to efficient
470 grinding at the molars (Cox et al., 2012). Druzinsky (2010) determined that of all the masticatory
471 muscles, it is the anterior deep masseter that confers efficacious incisor bites in sciuromorphs.
472 Here, it is indicated that the IOZM provides efficiency in molar bites in hystricomorphs, without
473 substantially increasing strains across the skull or the magnitude of cranial deformation. This
474 may go some way to explaining why hystricomorphy has evolved convergently at least four
475 times within the rodents.

476

477 **ACKNOWLEDGEMENTS**
478 The author thanks Matt Lowe and Rob Asher (University Museum of Zoology, Cambridge) for
479 the loan of the specimen, and Sue Taft and Michael Fagan (Medical and Biological Engineering
480 Group, University of Hull) for microCT scanning. Thanks are due to Paul O'Higgins for help
481 with geometric morphometrics.

482

483 **REFERENCES**
484 **Baverstock H, Jeffery NS, Cobb SN. 2013.** The morphology of the mouse masticatory
485   musculature. *Journal of Anatomy* **223:** 46-60.
486 **Becht G. 1953.** Comparative biologic-anatomical researcher on mastication in some mammals.
487   *Proceedings of the Koninklijke Nederlandse Akademie van Wetenschappen. Series C* **56:**
488   508-526.
489 **Becerra F, Casinos A, Vassallo AI. 2013.** Biting performance and skull biomechanics of a
490   chisel-tooth digging rodent (*Ctenomys tuconax*; Caviomorpha; Octodontoidea). *Journal*
491   *of Experimental Zoology* **319A:** 74-85.
492 **Becerra F, Echeverría AI, Casinos A, Vassallo AI. 2014.** Another one bites the dust: bite force
493   and ecology in three caviomorph rodents (Rodentia, Hystricognathi). *Journal of*
494   *Experimental Zoology* **283A:** 220-232.
495 **Bramble DM. 1978.** Origin of the mammalian fedding complex: Models and mechanisms.
496   *Paleobiology* **4:** 271-301.

497 **Bright JA. 2012.** The importance of craniofacial sutures in biomechanical finite element models
498   of the domestic pig. *PLoS ONE* **7:** e31769.

499 **Byrd KE. 1981.** Mandibular movement and muscle activity during mastication in the guinea pig
500   (*Cavia porcellus*). *Journal of Morphology* **170:** 147-169.

501 **Cleuren J, Aerts P, De Vree F. 1995.** Bite and joint force analysis in *Caiman crocodilus*.
502   *Belgian Journal of Zoology* **125,** 79-94.

503 **Cornette R, Herrel A, Cosson, J-F, Poitevin F, Baylac M. 2012.** Rapid morpho-functional
504   changes among insular populations of the great white-toothed shrew. *Biological Journal*
505   *of the Linnean Society* **107:** 322-331.

506 **Cox PG, Fagan MJ, Rayfield EJ, Jeffery N. 2011.** Finite element modelling of squirrel, guinea
507   pig and rat skulls: using geometric morphometrics to assess sensitivity. *Journal of*
508   *Anatomy* **219:** 696-709.

509 **Cox PG, Jeffery N. 2011.** Reviewing the jaw-closing musculature in squirrels, rats and guinea
510   pigs with contrast-enhanced microCT. *Anatomical Record* **294:** 915-928.

511 **Cox PG, Jeffery N. 2015.** The muscles of mastication and the function of the medial pterygoid.
512   In: Cox PG, Hautier L, eds. *Evolution of the Rodents: Advances in Phylogeny, Functional*
513   *Morphology and Development.* Cambridge: Cambridge University Press, 350-372.

514 **Cox PG, Kirkham J, Herrel A. 2013.** Masticatory biomechanics of the Laotian rock rat,
515   *Laonastes aenigmamus*, and the function of the zygomaticomandibularis muscle. *PeerJ*
516   **1:** e160.

517 **Cox PG, Rayfield EJ, Fagan MJ, Herrel A, Pataky TC, Jeffery N. 2012.** Functional evolution
518   of the feeding system in rodents. *PLoS ONE* **7:** e36299.

519 **Cox PG, Rinderknecht A, Blanco RE. 2015.** Predicting bite force and cranial biomechanics in
520   the largest fossil rodent using finite element analysis. *Journal of Anatomy* **226:** 215-223.

521 **Crompton AW. 1963.** The evolution of the mammalian jaw. *Evolution* **17:** 431-439.

522 **Cuff, AR, Bright JA, Rayfield EJ. 2015.** Validation experiments on finite element models of an
523   ostrich (*Struthio camelus*) cranium. *PeerJ* **3:** e1294.

524 **Curtis N, Witzel U, Fitton LC, O'Higgins P, Fagan MJ. 2011.** The mechanical significance of
525   the temporal fasciae in *Macaca fascicularis*: an investigation using finite element
526   analysis. *Anatomical Record* **294:** 1178-1190.

527 **Davis DD. 1955.** Masticatory apparatus in the spectacled bear *Tremarctos ornatus*. *Fieldiana*
528   *(Zoology)* **37:** 25-46.

529 **Davis JL, Santana SE, Dumont ER, Grosse IR. 2010.** Predicting bite force in mammals: two-
530   dimensional *versus* three-dimensional lever models. *Journal of Experimental Biology*
531   **213:** 1844-1851.

532 **Druzinsky RE. 2010.** Functional anatomy of incisal biting in *Aplondontia rufa* and sciuromorph
533   rodents – Part 2: Sciuromorphy is efficacious for production of force at the incisors. *Cells*
534   *Tissues Organs* **192:** 50-63.

535 **Dumont ER, Davis JL, Grosse IR, Burrows AM. 2011.** Finite element analysis of performance
536   in the skulls of marmosets and tamarins. *Journal of Anatomy* **218:** 151-162.

537 **Fabre P-H, Hautier L, Dimitrov D, Douzery EJP. 2012.** A glimpse on the pattern of rodent
538   diversification: a phylogenetic approach. *BMC Evolutionary Biology* **12:** 88.

539 **Figueirido B, Tseng JZ, Serrano-Alarcón FJ, Martín-Serra A, Pastor JF. 2014.** Three-
540   dimensional computer simulations of feeding behaviour in red and giant pandas relate
541   skull biomechanics with dietary niche partitioning. *Biology Letters* **10:** 20140196.

542 **Fitton LC, Shi JF, Fagan MJ, O'Higgins P. 2012.** Masticatory loadings and cranial
543   deformation in *Macaca fascicularis*: a finite element analysis sensitivity study. *Journal of*
544   *Anatomy* **221:** 55-68.

545 **Fitton LC, Proa M, Rowland C, Toro-Ibacache V, O'Higgins P. 2015.** The impact of
546   simplifications on the performance of a finite element model of a *Macaca fascicularis*
547   cranium. *Anatomical Record* **298:** 107-121.

548 **Gingerich PD. 1979.** The human mandible: Lever, link or both? *American Journal of Physical*
549   *Anthropology* **51:** 135-138.

550 **Gorniak GC. 1977.** Feeding in golden hamsters, *Mesocricetus auratus*. *Journal of Morphology*
551   **154:** 427-458.

552 **Greaves WS, 1978.** The jaw lever system in ungulates: a new model. *Journal of Zoology* **184:**
553   271-285.

554 **Greaves WS. 1982.** A mechanical limitation on the position of the jaw muscles of mammals: the
555   one-third rule. *Journal of Mammalogy* **63:** 261-266.

556 **Greaves WS. 2000.** Location of the vector of jaw muscle force in mammals. *Journal of*
557   *Morphology* **243:** 293-299.

558 **Greaves WS. 2012.** *The Mammalian Jaw: A Mechanical Analysis*. Cambridge: Cambridge
559   University Press.

560 **Hautier L, Cox PG, Lebrun R. 2015.** Grades and clades among rodents: the promise of
561   geometric morphometrics. In: Cox PG, Hautier L, eds. *Evolution of the Rodents:*
562   *Advances in Phylogeny, Functional Morphology and Development.* Cambridge:
563   Cambridge University Press, 277-299.

564 **Hiiemae K.** 1971. The structure and function of the jaw muscles in the rat (*Rattus norvegicus* L.)
565   III. The mechanics of the muscles. *Zoological Journal of the Linnean Society* **50:** 111-
566   132.

567 **Kerr A. 2010.** *Introductory Biomechanics*. Edinburgh: Churchill Livingstone.

568 **Kupczik K, Dobson CA, Fagan MJ, Crompton RH, Oxnard CE, O'Higgins P. 2007.**
569   Assessing mechanical function of the zygomatic region in macaques: validation and
570   sensitivity testing of finite element models. *Journal of Anatomy* **210:** 41-53.

571 **Liu J, Shi L, Fitton LC, Phillips R, O'Higgins P, Fagan MJ. 2012.** The application of muscle
572   wrapping to voxel-based finite element models of skeletal structures. *Biomechanics and*
573   *Modeling in Mechanobiology* **11:** 35-47.

574 **López-Antoñanzas R. 2016.** Family Pedetidae (Springhares). In: Wilson DE, Lacher TE,
575   Mittermeier RA, eds. *Handbook of the Mammals of the World. Volume 6: Lagomorphs*
576   *and Rodents I.* Barcelona: Lynx Edicions, 280-287.

577 **Mansour RM, Reynik RJ. 1975.** *In vivo* occlusal forces and moments: I. Forces measured in
578   terminal hinge position and associated moments. *Journal of Dental Research* **54:** 114-
579   120.

580 **McCabe K, Henderson K, Pantinople J, Richards HL, Milne N. 2017.** Curvature reduces
581   bending strains in the quokka femur. *PeerJ* **5:** e3100.

582 **McIntosh AF, Cox PG. 2016.** The impact of gape on the performance of the skull in chisel-
583   tooth digging and scratch digging mole-rats (Rodentia: Bathyergidae). *Royal Society*
584   *Open Science* **3:** 160568.

585 **Offermans M, De Vree F. 1989.** Morphology of the masticatory apparatus in the springhare,
586   *Pedetes capensis*. *Journal of Mammalogy* **70:** 701-711.

587 **Offermans M, De Vree F. 1990.** Mastication in springhares, *Pedetes capensis*: A
588   cineradiographic study. *Journal of Morphology* **205 :** 353-367.

589 **Offermans M, De Vree F. 1993.** Electromyography and mechanics of mastication in the
590   springhare *Pedetes capensis* (Rodentia, Pedetidae). *Belgian Journal of Zoology* **123:** 231-
591   261.

592 **O'Hare LMS, Cox PG, Jeffery N, Singer ER. 2013.** Finite element analysis of stress in the
593   equine proximal phalanx. *Equine Veterinary Journal* **45:** 273-277.

594 **O'Higgins P, Cobb SN, Fitton LC, Gröning F, Phillips R, Liu J, Fagan MJ. 2011.**
595   Combining geometric morphometrics and functional simulation: an emerging toolkit for
596   virtual functional analyses. *Journal of Anatomy* **218:** 3-15.

597 **O'Higgins P, Milne N. 2013.** Applying geometric morphometrics to compare changes in size
598   and shape arising from finite elements analysis. *Hystrix* **24:** 126-132.

599 **Peinke DM, Brown CR. 2003.** Metabolism and thermoregulation in the springhare (*Pedetes*
600   *capensis*). *Journal of Comparative Physiology B* **173:** 347-353.

601 **Peinke DM, Brown CR. 2006.** Habitat use by the southern springhare (*Pedetes capensis*) in the
602   Eastern Cape Province, South Africa. *South African Journal of Wildlife Research* **36:**
603   103-111.

604 **Porro LB, Metzger KA, Iriarte-Diaz J, Ross CF. 2013.** *In vivo* bone strain and finite element
605   modelling of the mandible of *Alligator mississippiensis*. *Journal of Anatomy* **223:** 195-
606   227.

607 **Rayfield EJ. 2007.** Finite element analysis and understanding the biomechanics and evolution of
608   living and fossil organisms. *Annual Review of Earth and Planetary Science* **35:** 541-576.

609 **Richmond BG, Wright BW, Grosse I, Dechow PC, Ross CF, Spencer MA, Strait DS. 2005.**
610   Finite element analysis in functional morphology. *Anatomical Record Part A* **283A:** 259-
611   274.

612 **Ross CF, Berthaume MA, Dechow PC, Iriarte-Diaz J, Porro LB, Richmond BG, Spencer**
613   **MA, Strait D. 2011.** *In vivo* bone strain and finite-element modeling of the craniofacial
614   haft in catarrhine primates. *Journal of Anatomy* **218:** 112-141.

615 **Santana SE. 2015.** Quantifying the effect of gape and morphology on bite force: biomechanical
616   modelling and *in vivo* measurements in bats. *Functional ecology* **30:** 557-565.

617 **Satoh K. 1998.** Balancing function of the masticatory muscles during incisal biting in two murid
618   rodents, *Apodemus speciosus* and *Clethrionomys rufocanus*. *Journal of Morphology* **236:**
619   49-56.

620 **Satoh K. 1999.** Mechanical advantage of area of origin for the external pterygoid muscle in two
621   murid rodents, *Apodemus speciosus* and *Clethrionomys rufocanus*. *Journal of*
622   *Morphology* **240:** 1-14.

623 **Satoh K, Iwaku F. 2006.** Jaw muscle functional anatomy in northern grasshopper mouse,
624   *Onychomys leucogaster*, a carnivorous murid. *Journal of Morphology* **267:** 987-999.

625 **Satoh K, Iwaku F. 2009.** Structure and direction of jaw adductor muscles as herbivorous
626   adaptations in *Neotoma Mexicana* (Muridae, Rodentia). *Zoomorphology* **128:** 339-348.

627 **Sharp A. 2015.** Comparative finite element analysis of the cranial performance of four
628   herbivorous marsupials. *Journal of Morphology* **276:** 1230-1243.

629 **Spencer MA. 1998.** Force production in the primate masticatory system: electromrographic test
630   of biomechanical hypotheses. *Journal of Human Evolution* **34:** 25-54.

631 **Spencer MA. 1999.** Constraints on masticatory system evolution in anthropoid primates.
632   *American Journal of Physical Anthropology* **108:** 483-506.

633 **Thomason JJ, 1991.** Cranial strength in relation to estimated biting forces in some mammals.
634   *Canadian Journal of Zoology* **69:** 2326-2333.

635 **Toro-Ibacache V, Fitton LC, Fagan MJ, O'Higgins P. 2016.** Validity and sensitivity of a
636   human cranial finite element model: implications for comparative studies of biting
637   performance. *Journal of Anatomy* **228:** 70-84.

638 **Tseng ZJ, Flynn JJ. 2015.** Are cranial biomechanical simulation data linked to known diets in
639   extant taxa? A method for applying diet-biomechanics linkage models to infer feeding
640   capability of extinct species. *PLoS ONE* **10:** e0124020.

641 **Tsouknidas A, Jimenez-Rojo L, Karatsis E, Michailidas N, Mitsiadis TA. 2017.** A bio-
642   realistic finite element model to evaluate the effect of masticatory loadings on mouse
643   mandible-related tissues. *Frontiers in Physiology* **8:** 273.

644 **Turnbull WD. 1970.** Mammalian masticatory apparatus. *Fieldiana (Geology)* **18:** 147-356.

645 **van Spronsen PH, Weijs WA, Valk J, Prahl-Andersen B, van Ginkel FC. 1989.** Comparison
646   of jaw-muscle bite-force cross-sections obtained by means of magnetic resonance
647   imaging and high-resolution CT scanning. *Journal of Dental Research* **68:** 1765-1770.

648 **Weijs WA, Dantuma R. 1975.** Electromyography and mechanics of mastication in the albino
649   rat. *Journal of Morphology* **146:** 1-34.

650 **Wilson DE, Reeder DM. 2005.** *Mammal Species of the World*. Baltimore: Johns Hopkins Press.

651 **Wood AE. 1965.** Grades and clades among rodents. *Evolution* **19:** 115-130.

652 **Woods CA. 1972.** Comparative myology of jaw, hyoid and pectoral appendicular regions of
653   New and Old World hystricomorph rodents. *Bulletin of the American Museum of Natural*
654   *History* **147:** 115-198.

655

656 **FIGURE LEGENDS**

657 **Figure 1. FE model showing muscle attachment sites and vectors.** Skull of *Pedetes capensis*
658   shown in (A) lateral and (B) dorso-lateral view. Key: light green, IOZM; yellow, lateral
659   pterygoid; blue, masseter; orange, medial pterygoid; brown, posterior masseter; red,
660   temporalis; dark green, zygomaticomandibularis.

661

662 **Figure 2. Landmarks used in GMM analysis of skull deformations.** Reconstruction of skull
663   of *Pedetes capensis* in (A) dorsal, (B) ventral and (C) left lateral view. Landmarks 11-28
664   recorded on both sides of the skull. Landmark descriptions are given in Table S1.

665

666 **Figure 3. Mechanical advantage at each tooth predicted by FE model.** Abbreviations: I,
667   incisor; PM, premolar; M1, first molar; M2, second molar; M3, third molar. Key: purple
668   line with circle, model with all muscles; blue line with crosses, masseter removed; light
669   green line with diamonds, IOZM removed; dark green line with triangles, ZM removed;
670   orange line with squares, medial pterygoid removed. Models with posterior masseter,
671   temporalis and lateral pterygoid removed not shown.

672

673 **Figure 4. Predicted principal strains across the skull of *Pedetes capensis* during incisor and**
674   **first molar biting.** Left, maximum (ε_1) principal strain; right, minimum (ε_3) principal
675   strains. First line, model with all masticatory muscles included; second line, model with
676   IOZM excluded; third line, model with masseter excluded; fourth line, model with ZM
677   excluded.

678

679 **Figure 5. GM analysis of cranial deformations in *Pedetes capensis*.** Plot of the first two
680   principal components from a GM analysis of 46 landmarks and 41 models. Axes not to
681   scale. Cranial reconstructions indicate shape changes (x400) along axes.

Muscle forces applied to each side of the model.

PCSA and percentage activations of each muscle from Offermans & De Vree (1993).

1   **Table 1.** Muscle forces applied to each side of the model. PCSA and percentage activations of each
2   muscle from Offermans & De Vree (1993).

	PCSA (cm²)	Maximum force (N)	% activation		Applied force (N)	
			Incision	Mastication	Incision	Mastication
Masseter	2.886	86.58	20	70	17.32	60.61
Posterior masseter	0.654	19.62	0	40	0.00	7.85
ZM	3.360	100.80	60	100	60.48	100.80
IOZM	2.244	67.32	100	60	67.32	40.39
Temporalis	0.516	15.48	0	30	0.00	4.64
Medial pterygoid	1.130	33.90	15	90	5.09	30.51
Lateral pterygoid	0.519	15.57	60	70	9.34	10.90

Bite force, joint reaction force and mechanical advantage of each model.

1   **Table 2.** Bite force, joint reaction force and mechanical advantage of each model.

	All muscles	No masseter	No posterior masseter	No ZM	No IOZM	No temporalis	No medial pterygoid	No lateral pterygoid
Bite force								
I	154.6	138.3	154.3	122.5	49.9	154.3	152.0	154.3
PM	347.5	244.4	345.7	247.4	232.5	346.6	319.9	348.7
M1	395.6	279.0	393.5	280.7	265.7	394.6	362.5	397.4
M2	457.7	323.0	455.2	324.7	307.8	456.4	418.8	459.8
M3	539.6	380.8	536.7	382.9	362.7	538.1	494.1	541.9
Joint reaction force								
I	85.9	83.0	86.2	39.8	56.0	86.2	79.3	154.3
PM	2.8	29.2	3.4	-2.3	38.8	-0.4	-26.9	9.3
M1	-45.3	-5.4	-44.4	-35.7	5.5	-48.3	-69.6	-39.5
M2	-107.3	-49.4	-106.1	-79.7	-36.4	-110.2	-125.9	-102.0
M3	-189.2	-107.1	-187.5	-137.9	-91.3	-191.8	-201.1	-184.0
Mechanical advantage								
I	0.64	0.62	0.64	0.75	0.47	0.64	0.66	0.50
PM	0.99	0.89	0.99	1.01	0.86	1.00	1.09	0.97
M1	1.13	1.02	1.13	1.15	0.98	1.14	1.24	1.11
M2	1.31	1.18	1.30	1.33	1.13	1.32	1.43	1.28
M3	1.54	1.39	1.54	1.56	1.34	1.55	1.69	1.51

Figure 1

FE model showing muscle attachment sites and vectors.

Skull of *Pedetes capensis* shown in (A) lateral and (B) dorso-lateral view. Key: light green,

IOZM; yellow, lateral pterygoid; blue, masseter; orange, medial pterygoid; brown, posterior

masseter; red, temporalis; dark green, zygomaticomandibularis.
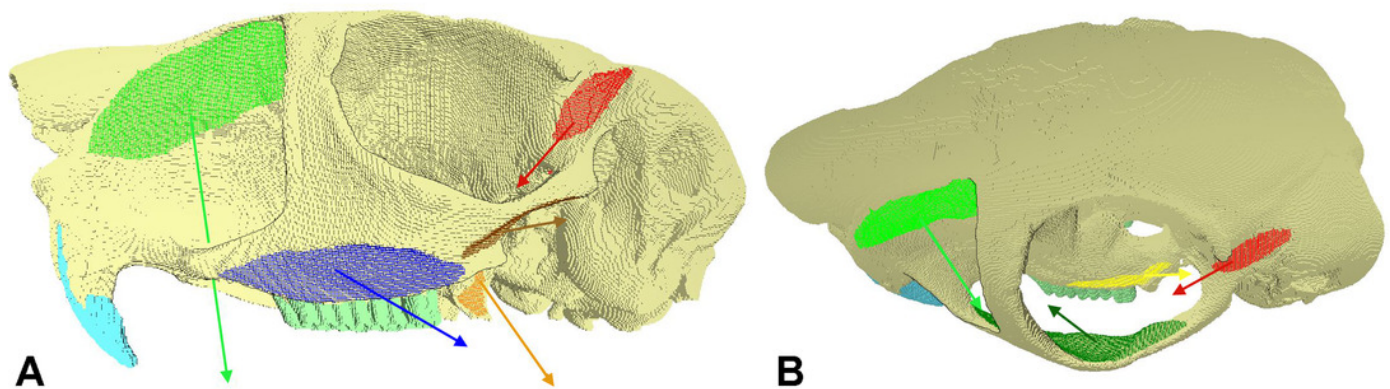
Figure 2

Landmarks used in GMM analysis of skull deformations.

Reconstruction of skull of *Pedetes capensis* in (A) dorsal, (B) ventral and (C) left lateral view. Landmarks 11-28 recorded on both sides of the skull. Landmark descriptions are given in Table S1.
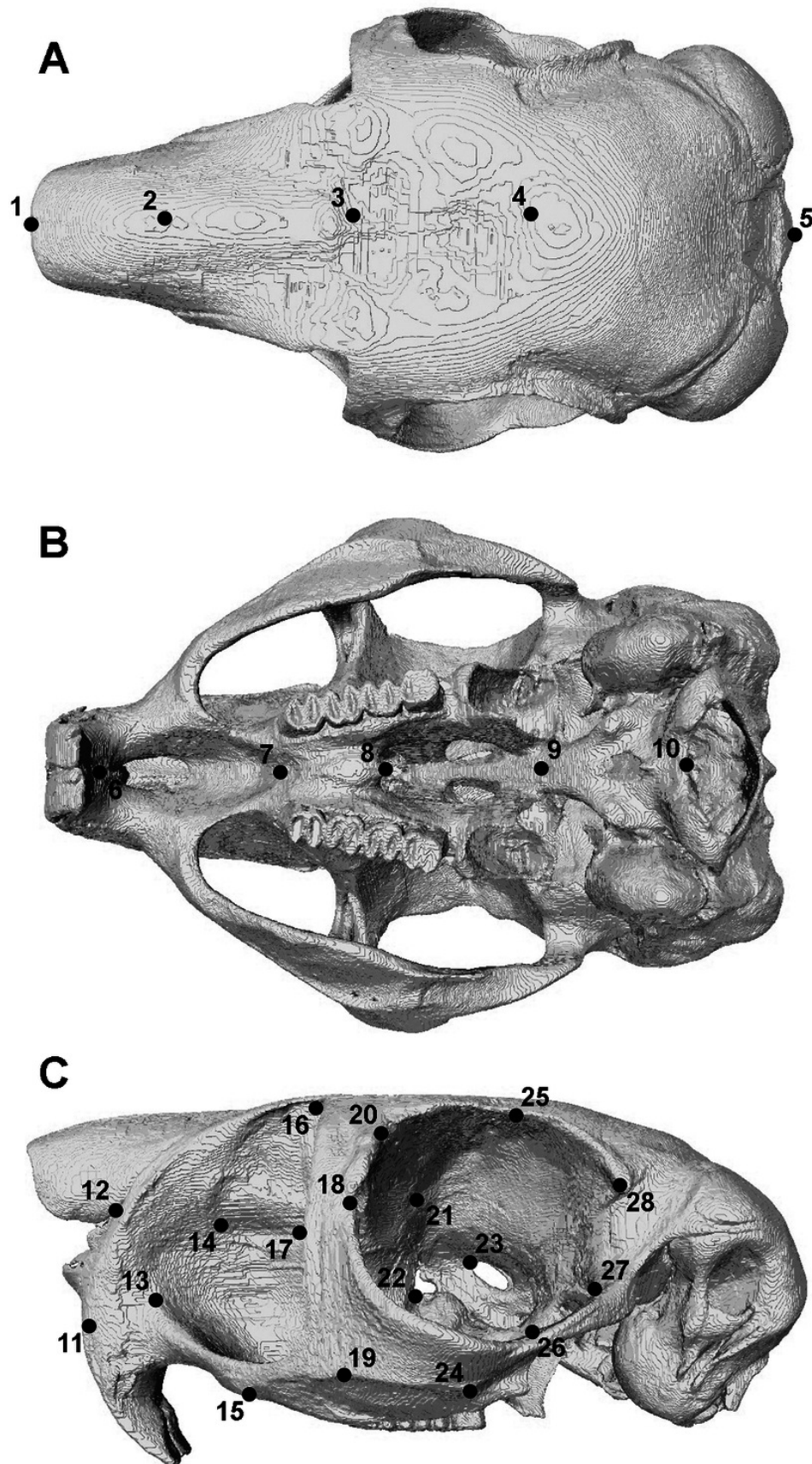
Figure 3

Mechanical advantage at each tooth predicted by FE model.

Abbreviations: I, incisor; PM, premolar; M1, first molar; M2, second molar; M3, third molar. Key: purple line with circle, model with all muscles; blue line with crosses, masseter removed; light green line with diamonds, IOZM removed; dark green line with triangles, ZM removed; orange line with squares, medial pterygoid removed. Data for models with posterior masseter, temporalis and lateral pterygoid removed available in Table 2 but not illustrated here.
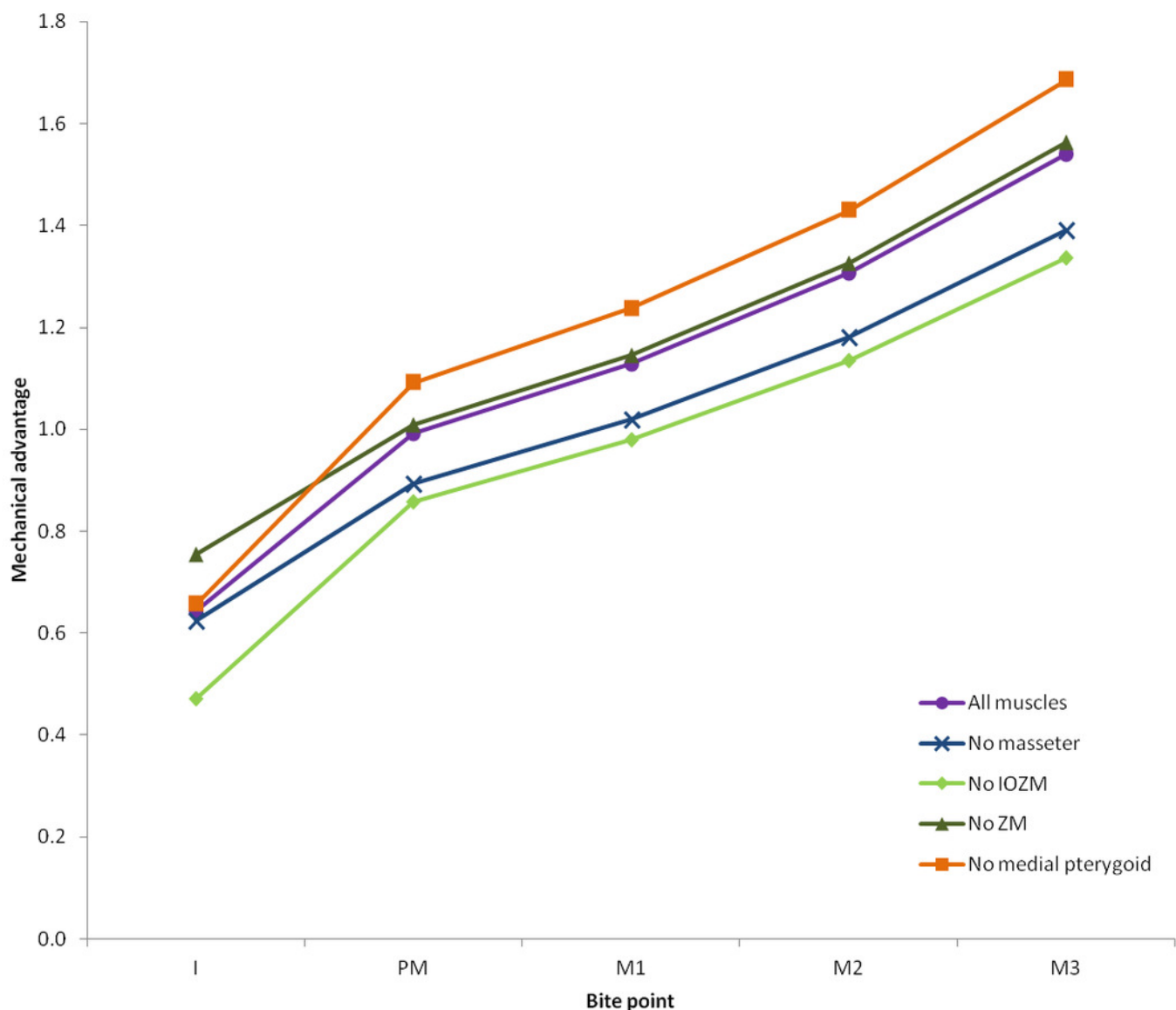
Figure 4

Predicted principal strains across the skull of *Pedetes capensis* during incisor and first molar biting.

A-H: maximum (ε_1) principal strains during incisor (A-D) and M1 (E-H) biting; I-P: minimum (ε_3) principal strains during incisor (I-L) and M1 (M-P) biting. A,E,I,M: model with all masticatory muscles included; B,F,J,N: model with IOZM excluded; C,G,K,O: model with masseter excluded; D,H,L,P: model with ZM excluded.
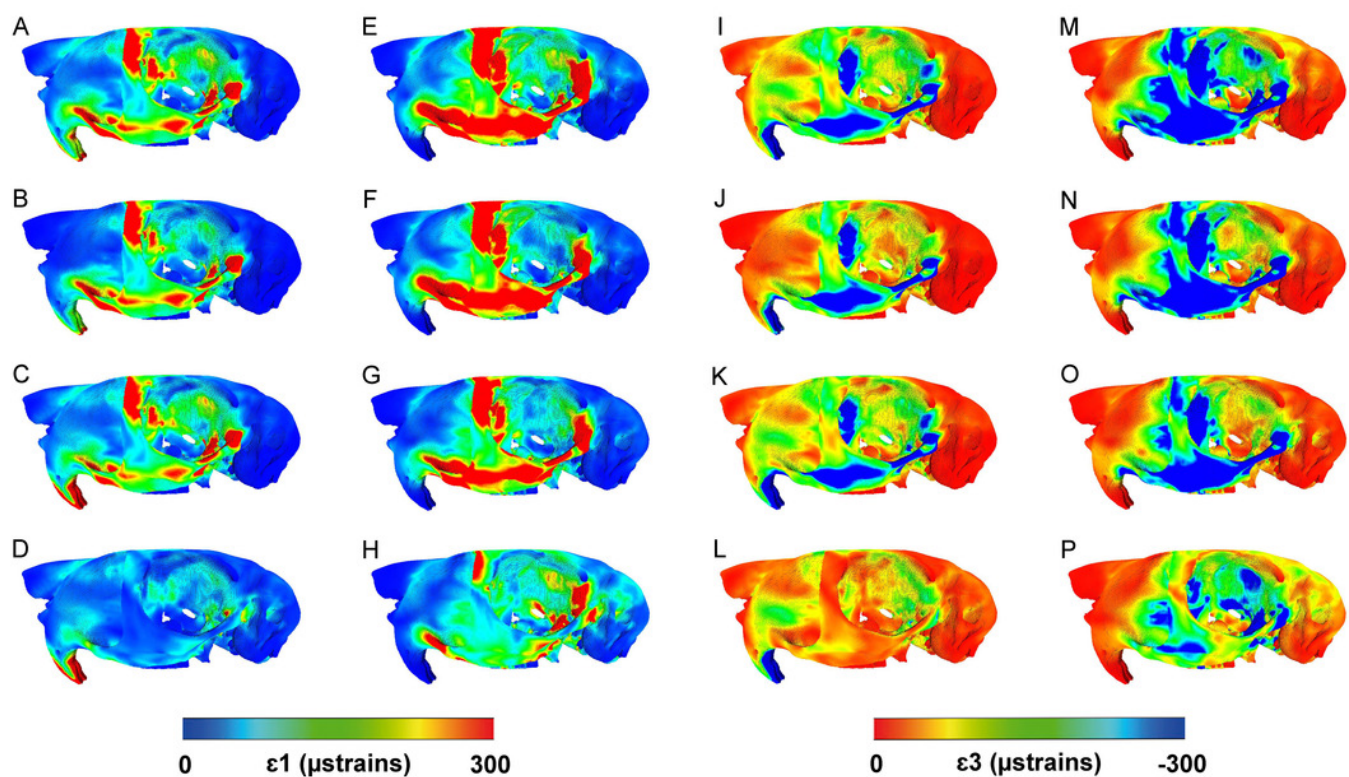
Figure 5

GM analysis of cranial deformations in *Pedetes capensis*.

Plot of the first two principal components from a GM analysis of 46 landmarks and 41 models.
Axes not to scale. Cranial reconstructions indicate shape changes (x400) along axes.